Check for updates

View Article Online
View Journal

NJC
New Journal of Chemistry

A journal for new directions in chemistry

Accepted Manuscript

This article can be cited before page numbers have been issued, to do this please use: B. Wu, H. Chang, Y. Liao and M. Yeh, *New J. Chem.*, 2020, DOI: 10.1039/D0NJ05172A.

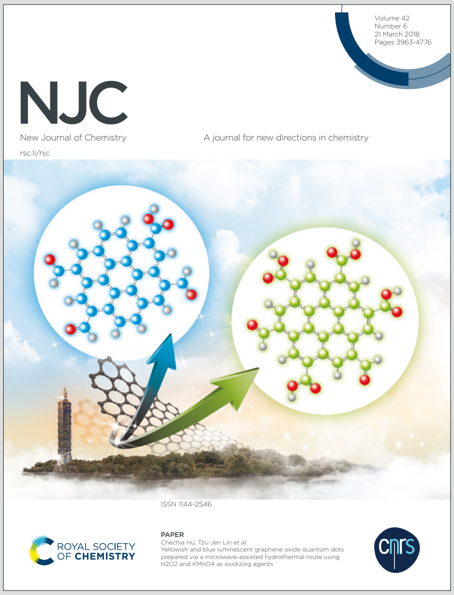

Volume 42
Number 6
21 March 2018
Pages 3963-4776

NJC
New Journal of Chemistry
A journal for new directions in chemistry
rsc.li/njc

ISSN 1144-2546

ROYAL SOCIETY OF CHEMISTRY

PAPER
Chechia Hu, Tzu-Jen Lin *et al.*
Yellowish and blue luminescent graphene oxide quantum dots prepared via a microwave-assisted hydrothermal route using H2O2 and KMnO4 as oxidizing agents

cnrs

This is an Accepted Manuscript, which has been through the Royal Society of Chemistry peer review process and has been accepted for publication.

Accepted Manuscripts are published online shortly after acceptance, before technical editing, formatting and proof reading. Using this free service, authors can make their results available to the community, in citable form, before we publish the edited article. We will replace this Accepted Manuscript with the edited and formatted Advance Article as soon as it is available.

You can find more information about Accepted Manuscripts in the Information for Authors.

Please note that technical editing may introduce minor changes to the text and/or graphics, which may alter content. The journal's standard Terms & Conditions and the Ethical guidelines still apply. In no event shall the Royal Society of Chemistry be held responsible for any errors or omissions in this Accepted Manuscript or any consequences arising from the use of any information it contains.

ROYAL SOCIETY OF CHEMISTRY

rsc.li/njc

View Article Online
DOI: 10.1039/D0NJ05172A

ARTICLE

Synthesis, Photochemical Isomerization and Photophysical Properties of Hydrazide-Hydrazone Derivatives

Received 00th January 20xx,
Accepted 00th January 20xx

DOI: 10.1039/x0xx00000x

Bao-Xing Wu, Hsin-Yueh Chang, Yi-Shun Liao and Mei-Yu Yeh*

The hydrazide-hydrazone derivatives have been utilized in molecular switches, sensing, metallo-assemblies, drug as well as other applications. The hydrazide-hydrazone functional group contains the -CO-NH-N=CH- moiety that gives the hydrazide-hydrazone group its physical, chemical and biochemical properties, however, the application in security protection have not been explored before. Herein, the ortho-, meta-, para-substituted pyridine conjugated to 2,6-dihydroxybenzoic acid, which containing hydrazide-hydrazone as photoswitch linker were designed and synthesized (**3a**-**3c**). Interestingly, when irradiation the ortho-substituted pyridine of molecule **3a** with 365 nm light, obvious emission intensity enhancements were detected. In contrast, **3a**-**3c** before irradiation and **3b**-**3c** after irradiation show no fluorescence. UV-Vis, fluorescence, ^{1}H NMR and Fourier transform infrared spectra as well as density functional theory calculations were carried out, which revealed that the hydrazide-hydrazone derivative of **3a** could undergo a characteristic *E* to *Z* photoisomerization after 365 nm light irradiation. The *Z* isomer of **3a** may have additional intramolecular hydrogen bond to restrict the motions of molecule, thus increasing the fluorescence intensity of **3a**. The experimental and molecular calculation results agreed well and thus demonstrated the first example of invisible ink based on the hydrazide-hydrazone motif.

1. Introduction

The hydrazide-hydrazone derivatives, which play an important role in organic synthesis, supramolecular chemistry and medicine chemistry, have been utilized in molecular switches, sensing, metallo-assemblies, drug as well as other applications.[1-9] The hydrazide-hydrazone functional group contains the -CO-NH-N=CH- moiety that has (i) the imine (C=N) double bond to exhibit *E*/*Z* isomerism and photochromism both in solution and in the solid state,[10-12] (ii) the coexistence of C=N and carbonyl (C=O) groups that improve the coordination capability of metal ions,[13-15] (iii) the NH and/or C=O groups provide the hydrogen bonds to bind the appropriate anions/cations and biomolecules,[16,17] and thus enables its use in various fields. These structural motifs give the hydrazide-hydrazone group its physical, chemical and biochemical properties, however, the application in invisible inks have not been explored.

Invisible inks can't be seen by the naked eye under normal conditions, until it is treated with chemicals, light, heat and acid/base.[18-21] In recent years, the materials with stimuli-responsive characteristics, such as pH, light, temperature, magnetic field etc., have been investigated widely and also have proven potential applications in security protection.[22-28] These smart materials can alteration their output response through external stimulation, making them possible to prevent the information being forged. Wang and Zheng have developed a new type of hydrochromic molecules as a double-encryption of invisible inks.[24] Kalita and coworkers reported a rewritable fluorescent ink and confirm its practical efficacy on various substrates by using acid/base vapors.[25] Ray et al. designed white light-emitting materials that show afterglow and invisible security ink.[26] Xu et al. established a photoresponsive fluorescent ink by aggregation-induced photodimerization of alkynylpyrene derivative.[27]

In this work, as shown in Scheme 1, the ortho-, meta-, para-substituted pyridine conjugated to 2,6-dihydroxybenzoic acid, which containing hydrazide-hydrazone as photoswitch linker were designed and synthesized (**3a**-**3c**). After 365 nm light irradiation, we found that the ortho-substituted pyridine of molecule **3a** may have additional intramolecular hydrogen bond to stabilize its *Z* isomer and restrict the motions of molecule, thus increasing the fluorescence intensity of **3a**. Herein, the structure-property-function relationships for these new materials are analyzed by various spectroscopies, e.g. UV-Vis, fluorescence, ^{1}H NMR and Fourier transform infrared spectra. Additionally, the molecular calculation studies of **3a**-**3c** can provide deep insights into the structure and dynamics of photoisomerization at the atomic level, which is essential to understand and ultimately manipulate their function. The experimental and molecular calculation results agreed well

---

[a] *Department of Chemistry, Chung Yuan Christian University, 200 Chung Pei Road, Chung-Li, Taiwan.*
E-mail: myyeh@cycu.edu.tw

† Footnotes relating to the title and/or authors should appear here.
Electronic Supplementary Information (ESI) available: [details of any supplementary information available should be included here]. See DOI: 10.1039/x0xx00000x

View Article Online
DOI: 10.1039/D0NJ05424A

and thus demonstrated the first example of invisible ink based on the hydrazide-hydrazone motif.

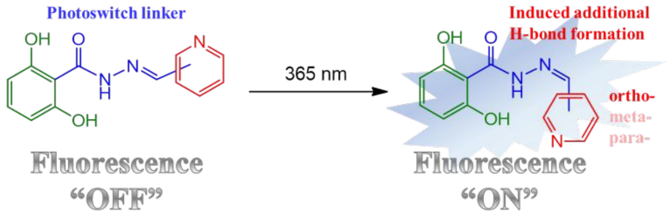

Scheme 1 Molecular design of hydrazide-hydrazone derivatives.

2. Experimental section

2.1 Materials and Instrumentation

All chemicals and reagents were commercially available and used as received without further purification. Dimethyl sulphate (DMS) was purchased from SHOWA chemical. 2,6-Dihydroxybenzoic acid, hydrazine monohydrate and *p*-toluenesulfonic acid (*p*-TsOH) were purchased from Alfa Aesar. 2-Pyridinecarboxaldehyde, 3-pyridinecarboxaldehyde, 4-pyridinecarboxaldehyde and methanol were obtained from Acros Organics. ^{1}H and ^{13}C NMR spectra were measured on a Bruker AVANCEII 400 NMR spectrometer using DMSO-d_6 as solvent. UV-Vis spectra were recorded on a Shimadzu UV-2550 spectrometer, fluorescence emission spectra were measured on a Shimadzu RF-1501 fluorescence spectrophotometer and Fourier transform infrared (FT-IR) spectra were obtained on Jasco 4600 FT/IR infrared spectrophotometer.

2.2 Synthesis

Synthesis of 2,6-dihydroxy benzohydrazide (**2**): Compound **2** was synthesized and purified according to literature procedure.[9] To the stirred solution of 2,6-dihydroxybenzoic acid (0.5 g, 3.25 mmol), DMS (0.28 mL, 2.9 mmol), potassium carbonate (0.45 g, 3.3 mmol) in 10 mL of acetone. After reaction at 55◦C for 24 hrs, the mixture was filtered off and the acetone was evaporated by rotary evaporator. The residue was extracted with ethyl acetate (3 x 25 mL), and the combined organic phase was dried with anhydrous magnesium sulfate and concentrated to give crude compound **1**. Subsequently, compound **1** was dissolved in 10 mL methanol (MeOH) and hydrazine monohydrate (1.5 mL, 29.8 mmol) was added dropwise in the above solution for 2 hrs. After the reaction, MeOH was evaporated and the crude product was purified by silica column chromatography to obtain compound **2** in 55% overall yield.

Synthesis of hydrazide-hydrazone molecules (**3a**-**3c**): 2-Pyridinecarboxaldehyde (41.6 mg, 0.39 mmol) and catalytic amount of *p*-TsOH were added to a solution of compound **2** (100 mg, 0.39 mmol) in 1.5 mL absolute ethanol (EtOH) with stirring at room temperature for overnight. The reaction mixture was concentrated and purified by silica column chromatography to yield (*E*)-2,6-dihydroxy-N'-(pyridin-2-ylmethylene)benzohydrazide (**3a**) in 66% yield. ^{1}H NMR (400 MHz, DMSO-d_6): δ= 6.40 (d, *J*= 8.1 Hz, 2H), 7.17 (t, *J*= 8.1 Hz, 1H), 7.41-7.44 (m, 1H), 7.87-7.91 (m, 1H), 7.96-7.98 (m, 1H), 8.39 (s, 1H), 8.62 (s, 1H), 11.73 (s, 2H), 11.90 (s, 1H). ^{13}C NMR (100 MHz, DMSO-d_6): δ=104.89, 107.55, 120.68, 125.04, 133.90, 137.42, 149.34, 150.05, 153.51, 159.72. HRMS (ESI) m/z for $C_{13}H_{12}N_3O_3$ [M+H]$^+$, calcd. 258.08787, found 258.08988.

In a manner similar to that described above, a mixture of 3-pyridinecarboxaldehyde (41.6 mg, 0.39 mmol), catalytic amount of *p*-TsOH and compound **2** (100 mg, 0.39 mmol) was converted to **3b** (60%). ^{1}H NMR (400 MHz,DMSO-d_6): δ= 6.43 (d, *J*= 8.2 Hz, 2H), 7.22 (t, *J*= 8.2 Hz, 1H), 7.49-7.53 (m, 1H), 8.14-8.17 (m, 1H), 8.48 (s, 1H), 8.63-864 (m, 1H), 8.85 (s, 1H), 11.88 (s, 1H), 12.03 (s, 2H). ^{13}C NMR (100 MHz, DMSO-d_6): δ= 104.02, 107.69, 124.54, 130.46, 134.13, 134.16, 147.01, 149.38, 151.40, 160.05, 166.51. HRMS (ESI) m/z for $C_{13}H_{12}N_3O_3$ [M+H]$^+$, calcd. 258.08787, found 258.08740.

In a manner similar to that described above, a mixture of 4-pyridinecarboxaldehyde (41.6 mg, 0.39 mmol), catalytic amount of *p*-TsOH and compound **2** (100 mg, 0.39 mmol) was converted to **3c** (79%). ^{1}H NMR (400 MHz, DMSO-d_6): δ= 6.41 (d, *J*= 8.2 Hz, 2H), 7.19 (t, *J*= 8.2 Hz, 1H), 7.66 (d, *J*= 6.1 Hz, 2H), 8.40 (s, 1H), 8.66 (*d*, J=6.1 Hz, 2H), 11.85 (s, 2H), 11.92 (s, 1H). ^{13}C NMR (100 MHz, DMSO-d_6): δ= 104.42, 107.66, 121.59, 134.16, 141.76, 147.10, 150.76, 159.92, 166.57. HRMS (ESI) m/z for $C_{13}H_{12}N_3O_3$ [M+H]$^+$, calcd. 258.08787, found 258.08774.

2.3 Computational Methodology

Geometry optimization and the theoretical electrostatic potential maps were performed through density functional theory (DFT) using B3LYP methods (Becke's three-parameter hybrid functional using the correlation functional of Lee, Yang, and Parr, which includes both local and non-local terms correlation functionals) at the 6-31G(d) level.[29, 30] The highest occupied molecular orbital- lowest unoccupied molecular orbital (HOMO-LUMO) analysis has been performed to explain the charge transfer place within the molecule.[30] Potential energy curves (PEC) were constructed starting from the *E* optimized geometry by constraining the N–N=C–C dihedral angle while optimizing all the other structural parameters. The constrained angle was incremented in 20◦ steps, between the *E* and *Z* minima, and the energy of the optimized structure obtained at each point.

3. Results and discussion

3.1 Synthesis of hydrazide-hydrazone molecules

The ortho-, meta-, para-substituted pyridine conjugated to 2,6-dihydroxybenzoic acid, which containing hydrazide-hydrazone as photoswitch linker were designed. The three new compounds of hydrazide-hydrazone derivatives (**3a**-**3c**) of this study were synthesized according to modified literature procedures.[7-9, 31, 32] Scheme 2 displayed the synthetic routes for these hydrazide-hydrazone derivatives of **3a**-**3c**.

View Article Online
DOI: 10.1039/D0NJ05172A

Compound **2** were synthesized from the reaction of 2,6-dihydroxybenzoic acid with DMS in the presence of potassium carbonate in acetone to obtain crude compound **1**. Without further purification, we then proceeded directly to the reaction of compound **1** with hydrazine monohydrate in MeOH to afford compound **2** in 55% two steps yield. 2-Pyridinecarboxaldehyde, 3-pyridinecarboxaldehyde, 4-pyridinecarboxaldehyde were reaction with compound **2** in the presence of *p*-TsOH in EtOH, respectively, to yield the hydrazide-hydrazone derivatives of **3a**-**3c** (60-79%).

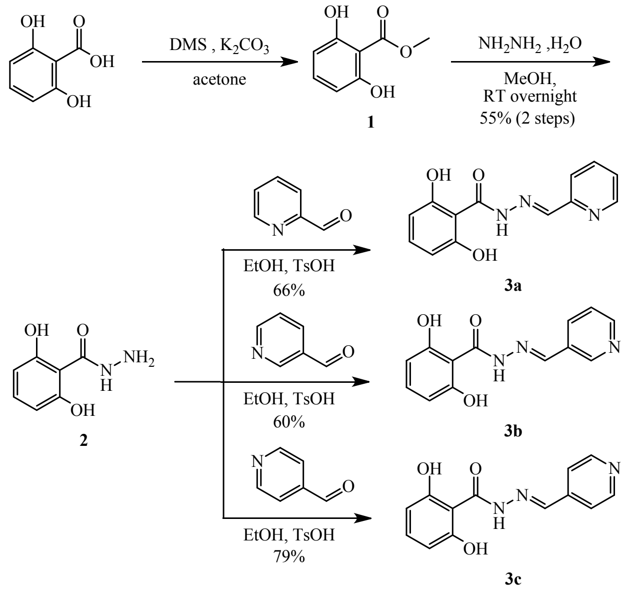

Scheme 2 Synthetic routes for hydrazide-hydrazone derivatives of **3a**-**3c**.

3.2 Photophysical Analysis and Characterization

UV-Vis absorption and fluorescence emission spectra of hydrazide-hydrazone derivatives of **3a**-**3c** at the concentration of 50 μM in DMSO are presented in Fig. 1, Fig. S1 and Fig. 2. As shown in Fig. 1 and Fig. S1, the absorption maximum for **3a**, **3b** and **3c** are ca. 322, 321 and 330 nm, respectively. We observed that when irradiation with 365 nm light for 5 hrs, the shapes of the absorption spectra changed in **3a**, while **3b** and **3c** almost retained their absorption features. The blue shift of the absorption spectrum of **3a** was obtained after irradiation, probably due to the photoisomerization of the *E* form to the *Z* form.[33] Fig. 2 displayed the fluorescence spectra of **3a**-**3c** with the excitation wavelength of their corresponding absorption maximum. Remarkably, among them, only **3a** revealed dramatically enhanced emission intensity after irradiation with 365 nm light. Furthermore, we compared the optical images of **3a**-**3c** under UV illumination, a bright blue light was detected in **3a** after 365 nm light irradiation, which is consistent with the observation of the fluorescence profile (Fig. 2 inset).

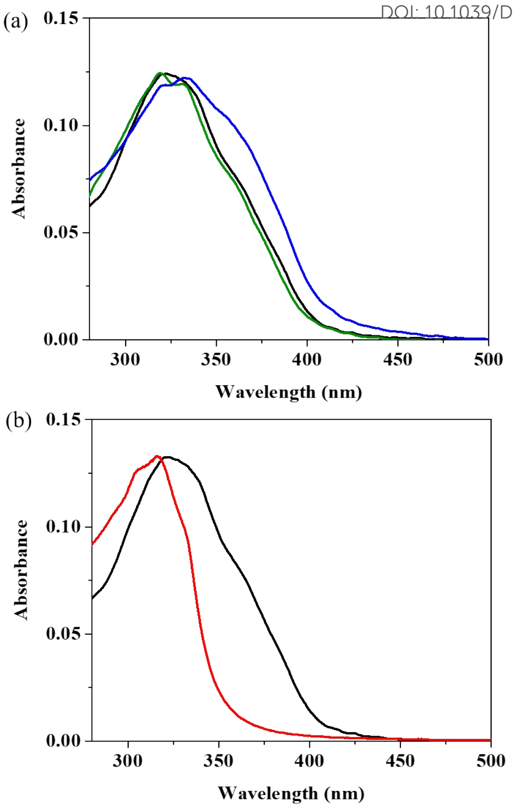

Fig. 1 UV-Vis absorption spectra of (a) **3a** (black), **3b** (green) and **3c** (blue) before irradiation and (b) **3a** before irradiation (black) and after irradiation (red) with 365 nm light in DMSO (Molecule concentration: 50 μM).

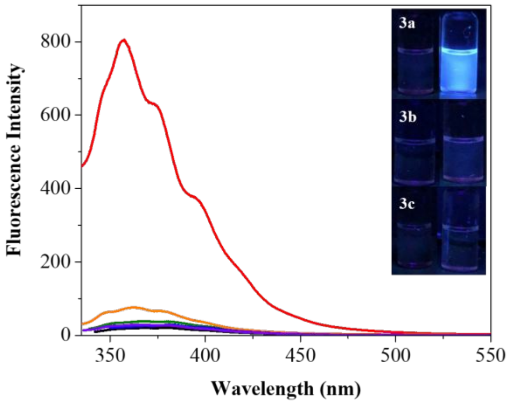

Fig. 2 Fluorescence spectra of **3a**, **3b** and **3c** before irradiation (black for **3a**, green for **3b**, blue for **3c**) and after irradiation (red for **3a**, orange for **3b**, purple for **3c**) with 365 nm light in DMSO (Molecule concentration: 50 μM). The inset showed the optical images of **3a**-**3c** taken under UV illumination (left: before irradiation; right: after irradiation).

To better understand the photophysical behavior of hydrazide-hydrazone derivatives of **3a**-**3c** (Fig. 1, Fig. S1 and Fig. 2), the photoisomerization was confirmed by ^{1}H NMR and FT-IR spectroscopies. Fig. 3 showed the ^{1}H NMR spectra of **3a**-**3c** before and after irradiation with 365 nm light. In the case of **3a**, we observed the hydrazone NH and HC=N protons at 11.90 and 8.39 ppm, respectively. Upon irradiation with 365 nm

View Article Online
DOI: 10.1039/D0NJ05173A

light, the downfield shift of NH proton (12.50 ppm) and an upfield shift of HC=N signal (7.76 ppm) were detected, which can be attributed to the *E* to *Z* photoisomerization (Fig. 3a and 3b).[34] FT-IR spectra of **3a** were depicted in Fig. 4 and the characteristic peaks at ca. 1550, 1650, 3305 cm^{-1} were assigned to C=N, C=O, and NH groups, respectively.[35] After irradiation, the NH signal was shifted to lowerwavenumber, indicating the formation of intramolecular hydrogen bonds in the *Z* isomer of **3a**.[36] This intramolecular hydrogen bond may restricted the rotation of the molecule, thus increasing the fluorescence intensity of **3a**.[9] In contrast, **3b** and **3c** didn't exhibit obvious changes in the ^{1}H NMR and FT-IR spectra before and after irradiation treatment compared to that of **3a** (Fig. 3c-3f and Fig. S2).

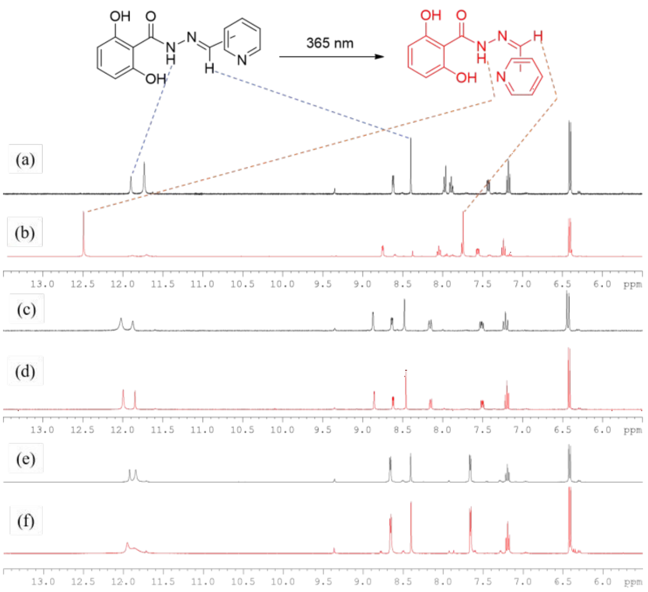

Fig. 3 Comparison of ^{1}H NMR spectra of (a, b) **3a**, (c, d) **3b** and (e, f) **3c** before irradiation (black) and after irradiation (red) with 365 nm light in DMSO-d_6.

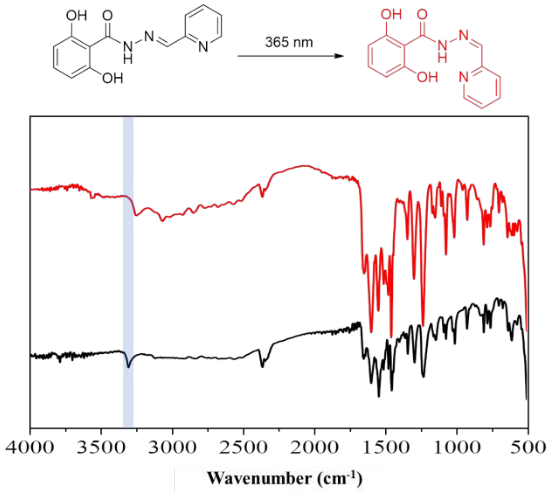

Fig. 4 Comparison of FT-IR spectra of **3a** before irradiation (black) and after irradiation (red) with 365 nm light in DMSO (Molecule concentration: 5,000 μM).

Since **3a** presented interesting photophysical properties, we further investigation the concentration effect on the UV-Vis absorption and fluorescence emission spectra of **3a** after 365 nm light irradiation. As shown in Fig. S3, we measured the absorption spectra of **3a** with different concentrations (50 μM, 500 μM and 5,000 μM). It was found that the absorption band at 375 nm increasingly strengthened with a gradual increase in the concentration of **3a**, suggesting that the ground state aggregates can be formed. Furthermore, the concentration dependence of the fluorescence spectra of **3a** were carried out with excitation wavelength at 315 nm (Fig. 5). It was observed that with increasing the concentration of **3a** from 50 μM to 5,000 μM, a red-shift emission peak from 356 to 379 nm and a new emission band around 450 nm appeared, which accompany the color changes in this optical images taken under UV illumination (Fig. 5 inset). For comparison, the optical images of **3a** before irradiation were also taken, showing that there is no fluorescence in the solution and solid states (Fig. S4 and S5). In addition, we have recorded the colors of **3a** at different concentrations without and with 365 nm light treatment, the yellow solution was observed at high concentration after 365 nm light irradiation taken under ambient room lighting (Fig. S6).

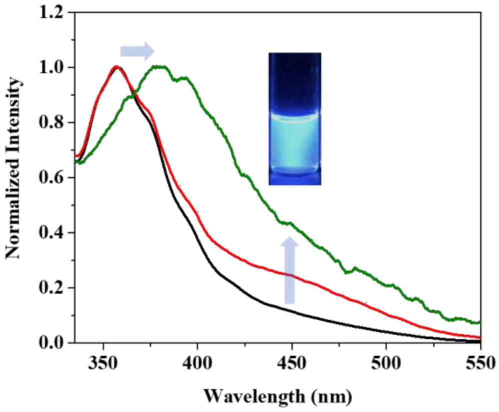

Fig. 5 Concentration dependence of fluorescence spectra of **3a** after irradiation with 365 nm light in DMSO (black for 50 μM, red for 500 μM and green for 5,000 μM). The inset showed the optical images of **3a** at high concentration taken under UV illumination.

Based on the above property of the compound **3a**, we attempt to use it on filter paper. We have manually written the word “CYCU” by using a DMSO solution of **3a**, as shown in Fig. 6a, after drying the filter paper, the word “CYCU” can't be found under ambient room lighting. Upon 365 nm light irradiation for a while, the word “CYCU” is visible by naked eye easily under both a visible light and a hand-held UV lamp (Fig. 6b and 6c). These experimental results are consistent with the observed photophysical properties of **3a**.

View Article Online
DOI: 10.1039/D0NJ05172A

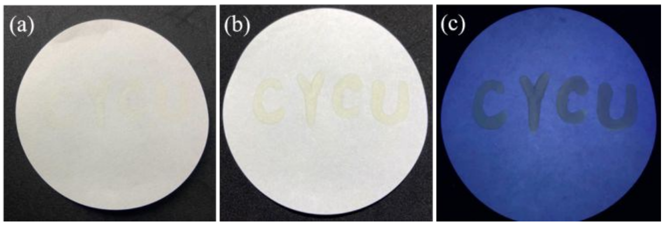

Fig. 6 Invisible ink experiment of **3a** (a) before irradiation and (b) after irradiation taken under ambient room lighting and (c) after irradiation taken under UV illumination.

3.3 Molecular Calculation

Molecular orbitals (HOMO-LUMO) and their properties such as electron distributions and energy are very useful for researchers to predict photochemical processes, chemical stability, photophysical properties and so on.[37-40] The energy diagram of frontier molecule orbital (eV) as well as the HOMO and LUMO energy of **3a**, **3b** and **3c** calculated by DFT/B3LYP/6-31G(d) method is shown in Fig. 7. The calculated energy band gaps are 4.19 eV (**3a**), 4.23 eV (**3b**) and 4.10 eV (**3c**), which are in excellent agreement with the experimental photophysical results. Moreover, we compared the difference between the electron distributions in HOMO and LUMO orbitals (**3a**-**3c**) and only significant electron density shift from the dihydroxybenzoic group to pyridine moiety in **3c**, indicating that **3c** possessed good intramolecular charge transfer characteristics.

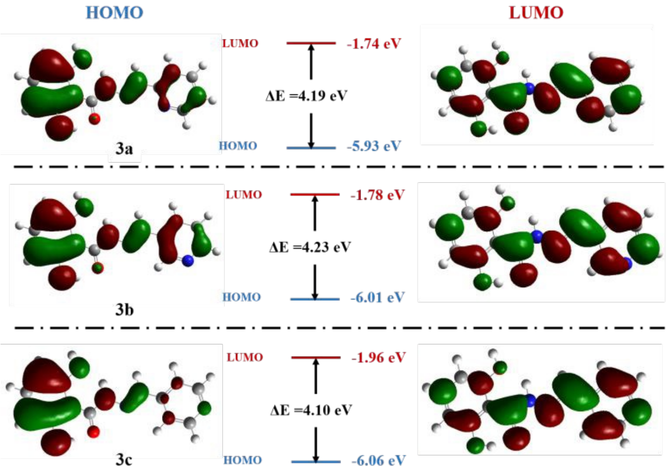

Fig. 7 Molecular orbital amplitude plots of HOMO and LUMO energy levels of **3a**, **3b** and **3c**, calculated by using DFT at the B3LYP/6-31G(d) level.

In order to provide more insight into the photochemical isomerization processes of hydrazide-hydrazone derivatives of **3a**-**3c**, the potential energy curves (PEC) and theoretical electrostatic potential maps were carried out.[41, 42] As can be seen from Fig. 8a and Fig. S7, the PEC of **3a**-**3c** were constructed by constraining the N-N=C-C dihedral angle to adopt fixed angles, from 180◦ to 0◦ degrees in 20◦ increments. The calculated relative energy barriers of **3a**-**3c** were 48.7, 49.8 and 50.1 kcal/mol, respectively. In addition, the calculated relative stabilities of the *Z* isomers were -4.5, 4.1, and 5.3 kcal/mol, respectively, indicating that **3a** has the most stable *Z* configuration. Fig. 8b displayed the optimized structures of *E* and *Z* isomers as well as transition state (TS) of **3a**-**3c**, we found that an intramolecular hydrogen bond can be formed in *Z* form of **3a**, suggesting the *Z* isomer has lower total energy than that of *E* isomer (Fig. S8, the distances of N-H···O and N-H···N are 1.94 Å and 2.04 Å, respectively). The visualization of the charge distributions and the electrostatic potential of **3a**-**3c** were shown Fig. 9. The calculation results indicated that negative electrostatic potentials were localized around the oxygen and nitrogen atoms of dihydroxybenzoic and pyridine moieties, resulting in higher electrostatic repulsion of **3a** and thus causing the rotation of the N-N bond between the two residues. These results imply that **3a** easily isomerizes to the *Z* isomer by irradiation of the *E* isomer. Additionally, we also calculated the absorption spectra of **3a-*E*** and **3a-*Z*** (Fig. S9), these results are comparable with the experimental data obtained in Fig. 1b. Overall, we systematically studied the effect of ortho-, meta-, para-substituted pyridine conjugated to 2,6-dihydroxybenzoic acid, which containing hydrazide-hydrazone as photoswitch linker, and investigated structure-property-function relationships. We concluded that when irradiation the ortho-substituted pyridine of molecule **3a** with 365 nm light may result additional intramolecular hydrogen bond to stabilize its *Z* isomer and restrict the motions of molecule, causing the strong emission peaks observed in **3a-*Z***.

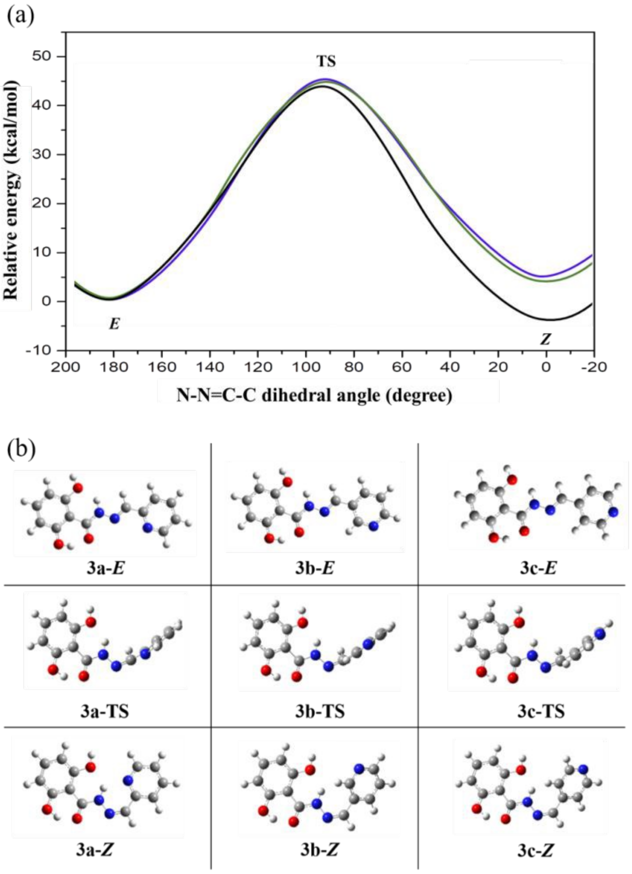

Fig. 8 (a) The computed potential energy curves for *E* to *Z* isomerization of **3a** (black), **3b** (green) and **3c** (blue) along a reaction coordinate corresponding to the N–N=C–C dihedral angle. (b) The optimized structures of *E* and *Z* isomers as well as TS of **3a**, **3b** and **3c**, calculated by using DFT at the B3LYP/6-31G(d) level.

View Article Online
DOI: 10.1039/D0NJ05172A

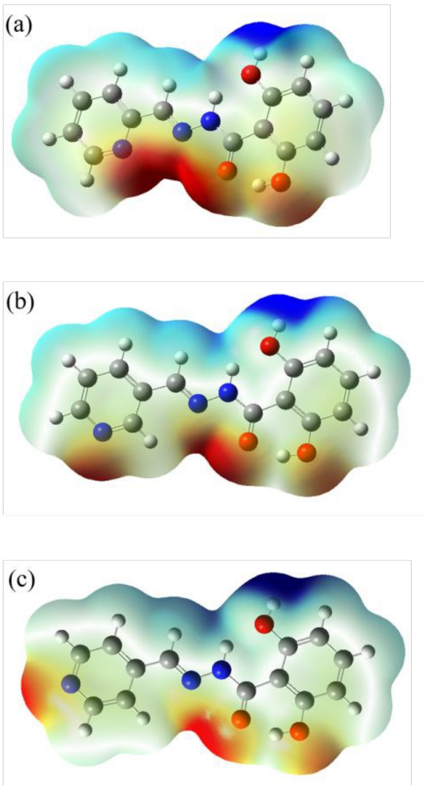

Fig. 9 3D representation of the electrostatic potentials around the molecules of (a) **3a**, (b) **3b** and (c) **3c**, determined using DFT at the B3LYP/6-31G(d) level.

4. Conclusions

In conclusion, the ortho-, meta-, para-substituted pyridine conjugated to 2,6-dihydroxybenzoic acid, which containing hydrazide-hydrazone as photoswitch linker were designed and synthesized (**3a**-**3c**). We found that only newly discovered hydrazide-hydrazone derivative of **3a** displayed strong fluorescence emission upon 365 nm light irradiation, while other didn't have any fluorescence. We studied the structure-property-function relationships for **3a**-**3c** through UV-Vis, fluorescence, ^{1}H NMR, FT-IR spectra as well as DFT calculations. The experimental and molecular calculation results indicated that the hydrazide-hydrazone derivative of **3a** could undergo a characteristic *E* to *Z* photoisomerization after 365 nm light irradiation. The *Z* isomer of **3a** may have additional intramolecular hydrogen bond to restrict the motions of molecule, thus illustrated the increasing the fluorescence intensity of **3a** and proven its potential application in security protection.

Conflicts of interest

There are no conflicts to declare.

Acknowledgements

This work was supported by the Ministry of Science and Technology of the Republic of China, Taiwan (MOST 109–2113-M-033-006-)

Notes and references

1 A. Coskun, M. Banaszak, R. D. Astumian,J. F. Stoddart and B. A. Grzybowski, *Chem. Soc. Rev.*, 2012, **41**, 19–30.
2 J. G. Hardy, *Chem. Soc. Rev.*, 2013, **42**, 7881–7899.
3 P. A. Gale, N. Busschaert, C. J. E. Haynes, L. E. Karagiannidis and I. L. Kirby, *Chem. Soc. Rev.*, 2014, **43**, 205–241.
4 S. Kobayashi, Y. Mori, J. S. Fossey and M. M. Salter, *Chem. Rev.*, 2011, **111**, 2626–2704.
5 J.-M. Lehn, *Angew. Chem. Int. Ed.*, 2013, **52**, 2836–2850.
6 X.-P. Zhou, Y. Wu and D. Li, *J. Am. Chem. Soc.*, 2013, **135**, 16062–16065.
7 V. Angelova, V. Karabeliov, A. Pavlina , A. Gateva, and J. Tchekalarova, *Drug Dev. Res.*, 2016, **77**, 379–392.
8 T. Nasr, S. Bondock, H. M. Rashed, W. Fayad, M. Youns and T. M. Sakr, *Eur. J. Med. Chem.*, 2018 , **151** ,723-739.
9 S. Patil, S. Pandey, A. Singh, M. Radhakrishna and S. Basu, *Chem. Eur. J.*, 2019, **25**, 8229 – 8235.
10 Y. E. Semenov, V. A. Smirnov, S. M. Aldoshin and B. G. Rogachev, *Russ. Chem. Bull.*, 2001, **50**, 2471–2472.
11 M. N. Chaur, D. Collado and J.-M. Lehn, *Chem. Eur. J.*, 2011, **17**, 248–258.
12 X. Su, S. Voskian, R. P. Hughes and I. Aprahamian, *Angew. Chem. Int. Ed.*, 2013, **52**, 10734–10739.
13 H. G. Wang, Y. P. Li, S. F. Xu, Y. C. Li, C. Zhou, X. L. Fei, L. Sun, C. Q. Zhang, Y. X. Li, Q. B. Yang and X. Y. Xu, *Org. Biomol. Chem.*, 2011, **9**, 2850–2855.
14 J.-c. Qin and Z.-y. Yang, *J. Photochem. Photobiol. A.*, 2016, **324**, 152–158.
15 H.-Q. Chang, L. Jia, J. Xu, W.-N. Wu, T.-F. Zhu, R.-H. Chen, T.-L. Ma, Y. Wang and Z.-Q. Xu, *Transit. Met. Chem.* 2015, **40**, 485–491.
16 H. Maniak, M. Talma, K. Matyja, A. Trusek and M. Giurg, *Molecules*, 2020, **25**, 1255.
17 H. Yang, H. S. Song, Y. C. Zhu and S. P. Yang, *Tetrahedron Lett.* , 2012, **53**, 2026–2029.
18 C. Sun, S. Su, Z. Gao, H. Liu, H. Wu, X. Shen and W. Bi, *ACS. Appl. Mater. Interfaces*, 2019, **11**, 8210–8216.
19 K. Liu, C. Shan, G. He, R. Wang, Z. Sun, Q. Liu, L. Dong and D. Shen, *J. Mater. Chem. C.*, 2017, **5**, 7167–7173.
20 W. Jeong, M. I. Khazi, D. Park, Y. Jung and J. Kim, *Adv. Funct. Mater.*, 2016, **26**, 5230–5238.
21 J. Andres, R. D. Hersch, J. E. Moser and A. S. Chauvin, *Adv. Funct. Mater.*, 2014, **24**, 5029–5036.
22 M. Irie, T. Fukaminato, T. Sasaki, N. Tamai and T. Kawai, *Nature*, 2002, **420**, 759–760.
23 B. Yoon, J. Lee, I. S. Park, S. Jeon, J. Lee and J. M. Kim *J. Mater. Chem. C.*, 2013, **1**, 2388–2403.
24 H. Zhao, X. Qin, L. Zhao, S. Dong, L. Gu, W. Sun, D. Wang and Y. Zheng, *ACS Appl. Mater. Interfaces*, 2020, **12**, 8952–8960.
25 A. Kalita, A. H. Malik and N. S. Sarma, *Chem. Asian J.*, 2020, **15**, 1074–1080.
26 H. Bhatia and D. Ray, *J. Phys. Chem. C.*, 2019, **123**, 22104–22113.
27 J. Zhang, S. X. Tang, R. Fu, X.D.Xu and S. Feng, *J. Mater. Chem. C.*, 2019, **7**, 13786-13793.
28 Y. Ni, Z. Sun, Y. Wang, H. F. Nour, A. C.-H. Sue, N. S. Finney, K.

View Article Online
DOI: 10.1039/D0NJ05172A

K. Baldridge and M. A. Olson, *J. Mater. Chem. C.*, 2019, **7**, 7399-7410.
29 K. B. Wiberg, *J. Comput. Chem.*, 1986, **7**, 379-379.
30 M. Drissi, N. Benhalima, Y. Megrouss, R. Rachida, A. Chouaih and F. Hamzaoui, *Molecules*, 2015, **20**, 4042-4054.
31 C. S. Manohar, A. Manikandan, P. Sridhar, A. Sivakumar, B. S. Kumar and S. R. Reddy, *J. Mol. Stru.*, 2018, **1154**, 437-444.
32 P. Sridhar, M. Alagumuthu, S. Arumugam and S. R. Reddy, *RSC Adv.*, 2016, **6**, 64460-64468.
33 E. L. Romero, R. F. D'Vries, F. Zuluaga and M. N. Chaur, *J. Braz. Chem. Soc.*, 2015, **26**, 1265-1273.
34 H. A. Abdel-Aziz, H. A. Ghabbour, W. M. Eldehna, M. M. Qabeel and H.-K. Fun, *J. Chem.*, 2014, **7**, 760434-760441.
35 L. Popiolek, *Med. Chem. Res.*, 2017, **26**, 287–301.
36 H. Rostkowska, M. J. Nowak, L. Lapinski and L. Adamowicz, *Phys. Chem. Chem. Phys.*, 2001, **3**, 3012-3017.
37 X. Li, G. Baryshnikov, C. Deng, X. Bao, B. Wu, Y. Zhou, H. Ågren and Li. Zhu, *Nat. Commun.*, 2019, **10**, 731.
38 R. Srivastava and L. R. Joshi, *Phys. Chem. Chem. Phys.*, 2014, **16**, 17284-17294.
39 J.-I. Aihar, *J. Phys. Chem. A.*, 1999, **103**, 7487-7495.
40 X.-Y. Xu, S. Lin, H. Xu, H. Guo and C. Zhao, *New J. Chem.*, 2020, **44**, 17222-17228.
41 T.-T. Yin, Z.-X. Zhao, L.-Y. Yu and H.-X. Zhang, *Org. Electron.*, 2017, **48**, 154-164.
42 Y. Ye, J. Pang, X. Zhou and J. Huang, *Comput. Theor. Chem.*, 2016, **1076**, 17-22.

View Article Online
DOI: 10.1039/D0NJ05172A

The structure-property relationships for the hydrazide-hydrazone derivatives were investigated to provide new insights into the design of photo-responsive materials